FACULTY OF MECHANICAL ENGINEERING

SUMMARY OF DISSERTATION

Preliminary version – 12th June 2007 – 14:01

Czech Technical University,
Faculty of Mechanical Engineering, Czech Republic

Von Karman Institute for Fluid Dynamics,
Sint-Genesius-Rode, Belgium

Université Libre de Bruxelles,
Bruxelles, Belgium

Summary of Ph.D. Thesis

Numerical Algorithms for the Computation of Steady and Unsteady Compressible Flow over Moving Geometries – Application to Fluid-Structure Interaction

Ing. Jiří Dobeš

Branch of Science:
Mathematical and Physical Engineering

Supervisors:
Prof. Jaroslav Fořt and Prof. Herman Deconinck

2007 Prague

Preliminary version – 12th June 2007 – 14:01

The thesis is an outcome of a full time joint Ph.D. study between the Czech Technical University, Faculty of Mechanical Engineering, Czech Republic and the Université Libre de Bruxelles, Bruxelles, Belgium. The research was carried out at the Von Karman Institute for Fluid Dynamics, Sint-Genesius-Rode, Belgium and at the Czech Technical University.

Ph.D. candidate:
Ing. Jiří Dobeš

Supervisors:
Prof. Jaroslav Fořt and Prof. Herman Deconinck

Opponents:
Prof. Gérard Degrez, Université Libre de Bruxelles, Belgium
Doc. Jiří Fürst, Czech Technical University, Prague
Dr. Mario Ricchuto, INRIA Futurs, France

This thesis was delivered on:
(FIXME: doplnit)

The defense of the dissertation will take place on:
(FIXME: opravit:) 15th of June 2007 in room No. 104, building D, ground floor of the Faculty of Mechanical Engineering, Czech Technical University, Karlovo náměstí 13, Praha 2 in front of the appointed *ad hoc* committee in the study program Mathematical and Physical Engineering. The thesis is available in the Department of Science and Research of Mechanical Engineering Faculty, Czech Technical University in Prague, Technická 4, Praha 6.

Prof. Karel Kozel
Head of Doctoral Study Program
Department of Technical Mathematics,
Faculty of Mechanical Engineering,
Czech Technical University,
Karlovo náměstí 13, Praha 2

Název práce: **Numerické metody pro výpočet stacionárního a nestacionárního stlačitelného proudění s uvažováním pohyblivých geometrií – s aplikací na interakce tekutiny s tělesy**

Anotace

Tato práce se zabývá vývojem numerických metod pro výpočty stlačitelného proudění s aplikací na interakci tekutiny a elastického tělesa.

Nejprve se zabýváme vývojem numerických metod založených na schématech využívajících distribuci residua (RD). Je presentován rozbor teoretických výsledků pro stabilitu a řád aproximace RD schémat. Reziduální schémata formulovaná pro řešení nestacionárních problémů jsou dále rozšířena pro případ výpočtů na časově proměnných sítích. Dále je pro řešení proudění vyvinuta metoda konečných objemů v cell centered i vertex centered formulaci. RD metoda je srovnána s metodou konečných objemů jednak teoreticky pomocí modifikované rovnice v jednorozměrném případě, tak i porovnáním numerických výsledků řešení skalární rovnice a systému Eulerových rovnic. Je presentováno množství dvou a trojrozměrných stacionárních i nestacionárních případů, dokládajících vlastnosti vyvinutých numerických metod. Výsledky jsou porovnány s teoretickým řešením a experimenty.

Ve druhé části disertační práce je vyvinuta numerická metoda pro řešení problémů interakce proudící tekutiny s tělesy. Problém je rozdělen na tři jednodušší problémy: problém dynamiky tekutin na pohyblivé výpočetní síti, problém pohybu tělesa a problém pohybu výpočetní sítě. Pohyb tělesa je popsán soustavou parciálních diferenciálních rovnic druhého řádu pro elastické anizotropní kontinuum a řešen metodou konečných prvků. Metoda je rozšířena pro výpočet vlastních kmitů tělesa. Pohyb sítě je formulován jako pohyb pseudo-elastického kontinua a opět řešen metodou konečných prvků. Uvedené tři problémy jsou spolu svázány iterační metodou. Vlastnosti metody jsou demonstrovány na případě 2D supersonického třepotání panelu (panel flutter) a 3D transsonického třepotání AGARD křídla. V prvním případě jsou výsledky srovnány s teoretickým řešením a výpočty publikovanými v literatuře, ve druhém případě s experimentem.

Abstract

Key words: Residual distribution scheme, Finite volume method, ALE method, Unsteady method, Implicit method, Parallel method, Unsteady flows, Aeroelasticity, Three field formulation, Finite element method, CFD, AGARD 445.6 wing, Panel flutter.

This work deals with the development of numerical methods for compressible flow simulation with application to the interaction of fluid flows and structural bodies.

First, we develop numerical methods based on multidimensional upwind residual distribution (RD) schemes. Theoretical results for the stability and accuracy of the methods are given. Then, the RD schemes for unsteady problems are extended for computations on moving meshes. As a second approach, cell centered and vertex centered finite volume (FV) schemes are considered. The RD schemes are compared to FV schemes by means of the 1D modified equation and by the comparison of the numerical results for scalar problems and system of Euler equations. We present a number of two and three dimensional steady and unsteady test cases, illustrating properties of the numerical methods. The results are compared with the theoretical solution and experimental data.

In the second part, a numerical method for fluid-structure interaction problems is developed. The problem is divided into three distinct sub-problems: Computational Fluid Dynamics, Computational Solid Mechanics and the problem of fluid mesh movement. The problem of Computational Solid Mechanics is formulated as a system of partial differential equations for an anisotropic elastic continuum and solved by the finite element method. The mesh movement is determined using the pseudo-elastic continuum approach and solved again by the finite element method. The coupling of the problems is achieved by a simple sub-iterative approach. Capabilities of the methods are demonstrated on computations of 2D supersonic panel flutter and 3D transonic flutter of the AGARD 445.6 wing. In the first case, the results are compared with the theoretical solution and the numerical computations given in the references. In the second case the comparison with experimental data is presented.

Contents

1 Introduction

A large number of methods is available for the solution of compressible flows today. They work on structured or unstructured meshes. Since structured mesh generation is one of the biggest bottlenecks for industrial type simulations, see e.g. [2], we will focus on methods working on unstructured meshes. One of the most commonly used methods for industrial type compressible flow simulations on unstructured meshes is the finite volume method in cell centered or vertex centered settings, see e.g. [12, 3]. Despite its large popularity, there are still some problems unresolved, namely accuracy for the flow features not aligned with the mesh, and dependence of the scheme on 1D physics introduced by the numerical flux.

As a cure to the above-mentioned problems, the residual distribution (RD) schemes were suggested in [20]. Since then, a successful development was sought. Nowadays, RD schemes can be used to solve complex problems such as 3D inviscid flows around full aircraft or 3D turbulent flow past a wing. A first objective of the thesis is to select several residual distribution schemes and to obtain their properties for well defined test cases. Then the schemes should be applied to technically important problems and problems of mathematical physics.

The fluid–structure interaction problems ultimately call for highly accurate methods. Since RD schemes are expected to be more accurate than traditional finite volume schemes, the use of RD methods for fluid–structure interaction problems is appealing. Until recently, only first order RD schemes for moving grids computations were available, see [14]. Hence, a second objective of the thesis is to explore possible extension of higher order accurate RD schemes for computations on moving meshes with application to aeroelastic simulations.

2 Specific objectives of the thesis

The goals of the presented work are:

1. To develop a numerical method based on selected schemes of residual distribution type and to analyse some of their properties. Eventually find possible improvements for particular flow problems. Develop an extension for problems involving a time dependent domain of solution.

2. To develop a numerical method based on a finite volume method in

cell centered or vertex centered formulation. Include the possibility of handling a time dependent domain of solution.

3. To test selected numerical methods on problems of scalar conservation law and system of Euler equations, with particular attention to the accuracy of the schemes and monotone capturing of complex solution features.

4. To develop a finite element method for the problem of elasticity, where the material is modeled as an elastic continuum allowing large displacements and taking into account possible anisotropic material properties.

5. To develop and validate the numerical method for fluid structure interaction problems, where the flow is modeled as a inviscid perfect gas and the body either as a elastic continuum or by a system of two ordinary differential equations.

3 Formulation of the fluid dynamics problem

The fluid dynamics problem is formulated in an Arbitrary Lagrangian Eulerian (ALE) frame of reference. We define the ALE mapping [9] which for each $t \in [0, t^{\max}]$ associates a point $\vec{Y}$ of reference configuration Ω_0 to a point $\vec{x}$ on the current domain configuration Ω_t, $\mathcal{A}_t : \Omega_0 \subset \mathbb{R}^d \mapsto \Omega_t \subset \mathbb{R}^d$, $\vec{x}(\vec{Y}, t) = \mathcal{A}_t(\vec{Y})$, where d is the number of spatial dimensions. The ALE mapping $\mathcal{A}_t$ is chosen sufficiently smooth and invertible with nonzero determinant of Jacobian $J_{\mathcal{A}_t}$. A domain velocity $\vec{w}(\vec{x}, t)$ is defined as the time derivative of $\vec{x}$ for constant $\vec{Y}$. We start from the conservative ALE formulation of the Euler equations in d spatial dimensions

$$\frac{1}{J_{\mathcal{A}_t}} \frac{\partial J_{\mathcal{A}_t} \mathbf{u}}{\partial t}\bigg|_{\vec{Y}} + \nabla_x \cdot [\vec{\mathbf{f}}(\mathbf{u}) - \mathbf{u}\vec{w}] = 0, \tag{1}$$

where the conserved variables are

$$\mathbf{u} = (\rho, \rho\vec{v}, E), \tag{2}$$

with density ρ, components of the velocity vector $\vec{v} = (v_1, \ldots, v_d)$ and total energy E. The flux is

$$\mathbf{f}_i = (\rho v_i, \rho v_i v_j + \delta_{ij} p, [E + p] v_i), \qquad 1 \le j \le d, \tag{3}$$

where p is the static pressure and δ_{ij} is Kronecker delta symbol. The system is closed by a thermodynamic equation of state for the pressure $p = f(\mathbf{u})$. We will only consider a perfect gas, then the equation is given by

$$p = (\gamma - 1)\left(E - \frac{1}{2}\rho \sum_{i=1}^{d} v_i^2\right). \tag{4}$$

The ratio of specific heats for a diatomic gas is used, i.e. $\gamma = 1.4$ (if not specified otherwise). The system is equipped with an entropy inequality. Equation (1) reduces to the standard system of conservation laws

$$\frac{\partial \mathbf{u}}{\partial t} + \nabla \cdot \vec{\mathbf{f}}(\mathbf{u}) = 0 \tag{5}$$

for a fixed mesh.

As a simplification, we will also consider a scalar conservation law, where $u : \mathbb{R}^d \to \mathbb{R}$ and $\vec{f} : \mathbb{R} \to \mathbb{R}^{d\times 1}$, in particular an advection equation, where the flux vector is defined as $\vec{f}(u; x, y) = (-yu, xu)$ in two dimensions and $\vec{f}(u; x, y, z) = (-yu, xu, 0)$ in the case of three dimensions.

The problem is closed with a set of initial and boundary conditions.

4 Residual distribution scheme

Several methods based on distribution of residuals have been developed in the past, see e.g. [15, 20], for a survey see e.g. [16]. This part of the work deals with residual distribution schemes as defined in [12], i.e. schemes, which are usually written as in section 4.1 and 4.2. Such schemes will be referred to as *residual distribution schemes*.

4.1 Introduction and general framework

We will consider meshes consisting of only simplex elements in this work. The residual distribution schemes for steady problems generally involve the following steps:

1. Compute the *residual* as the integral of the convective terms of equation (5) over element E as

$$\phi^E = \int_E \nabla \cdot \vec{\mathbf{f}}^h \, \mathrm{d}\vec{x} = -\int_E \frac{\partial \mathbf{u}^h}{\partial t} \, \mathrm{d}\vec{x} = \sum_{i\in E} \mathbf{k}_i \mathbf{u}_i, \tag{6}$$

where $i \in E$ means all the nodes in element E and

$$\mathbf{k}_j = \frac{\partial \vec{\mathbf{f}}^h}{\partial \mathbf{u}^h}(\bar{\mathbf{u}}) \cdot \frac{\vec{n}_j}{d} \tag{7}$$

is the upwind matrix. Symbol $\vec{n}_i$ denotes the normal perpendicular to the face opposite to the node i scaled by its measure. The state $\bar{\mathbf{u}}$ for the evaluation of the Jacobian is suitable chosen, see [5], such that the method is conservative.

2. *Distribute* the residual ϕ^E to the nodes of element E via distribution matrix β_i

$$\phi_i^E = \beta_i^E \phi^E, \quad \text{such that } \sum_{i \in E} \phi_i^E = \phi^E. \tag{8}$$

3. Update the solution in all the nodes of the computational domain

$$\mathbf{u}_i^{h,n+1} = \mathbf{u}_i^{h,n} - \alpha_i \sum_{E \in i} \phi_i^E, \tag{9}$$

where n is the index of the time level and $\alpha_i > 0$ is a relaxation parameter, to be specified later.

Certain schemes define directly the residual contribution ϕ_i^E to the node i. The distribution coefficient is then defined implicitly from eq. (8).

4.2 RD schemes for unsteady problems

The above-stated RD schemes are first order accurate at most for unsteady problems even if a high order time discretization scheme is used, see, e.g. [8]. The reason is that there exists a coupling between spatial and temporal discretization through a finite element type mass matrix. The accuracy problem was treated by two distinct approaches: schemes formulated using a mass matrix, see, e.g. [8] and space-time schemes, see, e.g. [1]. Although the schemes were derived using different frameworks, they can be reduced to a common base. Namely, we can formulate the unsteady problem (5) using the pseudo time stepping (or dual time), i.e.

$$\frac{\partial \mathbf{u}}{\partial \tau} + \frac{\partial \mathbf{u}}{\partial t} + \sum_{j=1}^{d} \frac{\partial}{\partial x_j} \mathbf{f}_j(\mathbf{u}) = \mathbf{0}, \tag{10}$$

and we seek for an unsteady solution of (5) as a steady solution of (10) in pseudoo time

$$\lim_{\tau\to\infty} \frac{\partial \mathbf{u}}{\partial \tau} = \mathbf{0}. \tag{11}$$

Hence we can proceed with a similar solution method as in section 4.1:

1. Compute the approximation of the *unsteady residual* as the integral of equation (5) over the space-time element E^{ST} between time levels n and $n+1$

$$\phi^{E^{\mathrm{ST}}} = \int_{E^{\mathrm{ST}}} \left(\frac{\partial \mathbf{u}^h}{\partial t} + \nabla \cdot \vec{\mathbf{f}}^h \right) \mathrm{d}\vec{x}\,\mathrm{d}t = \int_{[t^n, t^{n+1}]} \int_E \left(\frac{\partial \mathbf{u}^h}{\partial t} + \nabla \cdot \vec{\mathbf{f}}^h \right) \mathrm{d}\vec{x}\,\mathrm{d}t. \tag{12}$$

2. *Distribute* residual $\phi^{E^{\mathrm{ST}}}$ to the nodes of the element E^{ST} located on the time level $n+1$ via the distribution parameter (matrix) β_i

$$\phi_i^{E^{\mathrm{ST}}} = \beta_i^{E^{\mathrm{ST}}} \phi^{E^{\mathrm{ST}}} \quad \text{with} \quad \sum_{i\in E} \phi_i^{E^{\mathrm{ST}}} = \phi^{E^{\mathrm{ST}}}. \tag{13}$$

   Because we have an initial value problem with data at n, the distribution is constrained to nodes at $n+1$.

3. Update the solution in all the nodes of the computational domain at the time level $n+1$

$$\mathbf{u}_i^{h,n+1,m+1} = \mathbf{u}_i^{h,n+1,m} - \alpha_i \sum_{E\in i} \phi_i^{E^{\mathrm{ST}}}, \tag{14}$$

   where m is the index of the pseudo-time step and α_i is the relaxation coefficient.

4. The steps 1. to 3. are repeated until a steady solution in pseudo-time is found. Then, the next layer of the space-time elements is considered $[t^n, t^{n+1}] \to [t^{n+1}, t^{n+2}]$.

4.3 Some examples of considered numerical schemes

The core contribution of the thesis consists of novel extensions of the residual distribution schemes for moving meshes. We will present the extension of the second order LDA scheme and the first order N scheme. Then, we briefly explain the construction of two nonlinear schemes, the N-modified scheme and the Bx scheme.

LDA scheme is a second order accurate linear scheme. We will consider a scalar problem for a moment. For the LDA scheme we use an equivalency of the linearity preserving RD schemes with the Petrov-Galerkin FEM formulation. The solution and the mesh velocity are approximated by linear Galerkin trial functions ψ_i from the current domain configuration. The Petrov–Galerkin test function is given on each element E by $\varphi_i^E = \psi_i + \beta_i - 1/(d+1)$, where β_i is the RD distribution coefficient for node i. For the mesh velocity term we use $\nabla_x \cdot (\mathbf{u}\vec{w}) = \mathbf{u}\nabla_x \cdot \vec{w} + \nabla_x \mathbf{u} \cdot \vec{w}$ and the identity

$$\nabla_x \cdot \vec{w} = \frac{1}{J_{\mathcal{A}_t}} \frac{\partial J_{\mathcal{A}_t}}{\partial t}\bigg|_{\vec{Y}}. \tag{15}$$

These terms have to be treated carefully to retain conservativity of the scheme [14]. This formulation gives us the (semi-discrete) element contribution

$$\phi_i^{E,\mathrm{LDA}} = \frac{1}{J^h_{\mathcal{A}_t}} \sum_{j\in E} \frac{\partial J^h_{\mathcal{A}_t} u_j}{\partial t}\bigg|_{\vec{Y}} m_{ij}^E + \phi_i^{E,\mathrm{sLDA}} - \frac{1}{J^h_{\mathcal{A}_t}} \frac{\partial J^h_{\mathcal{A}_t}}{\partial t}\bigg|_{\vec{Y}} \left(\sum_{j\in E} u_j m_{ij}^E \right), \tag{16}$$

where $m_{ij}^E = \int_E \varphi_i \psi_j \,\mathrm{d}\vec{x}$ is the element contribution to the mass matrix and $\phi_i^{E,\mathrm{sLDA}}$ is the well known nodal contribution from the *steady* version of the LDA scheme

$$\beta_i = k_i^+ N \tag{17}$$

where $k^\pm = \pm \max(0, \pm k)$ and

$$N \equiv (\sum_{i\in E} k_i^+)^{-1}. \tag{18}$$

For the time discretization, the 3BDF formula is used, i.e. the ALE time derivative is approximated by

$$\frac{1}{J^h_{\mathcal{A}_t}} \frac{\partial J^h_{\mathcal{A}_t} u_j}{\partial t}\bigg|_{\vec{Y}} = \frac{\alpha^{n+1}\mu(E^{n+1})u_j^{n+1} + \alpha^n \mu(E^n) u_j^n + \alpha^{n-1}\mu(E^{n-1})u_j^{n-1}}{t^{n+1} - t^n} \tag{19}$$

with coefficients

$$\alpha^{n+1} = \frac{1+2\tau}{1+\tau}, \quad \alpha^n = -1-\tau, \quad \alpha^{n-1} = \frac{\tau^2}{1+\tau}, \quad \tau = \frac{t^{n+1}-t^n}{t^n - t^{n-1}}. \quad (20)$$

The measure (volume) of the element is denoted by $\mu(E)$. All the terms in (16) are evaluated at time level $n+1$.

The first order N scheme is formulated with diagonally lumped mass matrix, the geometric source term is divided into the convective part and the velocity divergence term, the latter treated by the point-wise discretization on the dual grid. The 3BDF time discretization is again used.

$$\phi_i^{E,\mathrm{N}} = \frac{\alpha^{n+1}\mu(E^{n+1})u_i^{n+1} + \alpha^n\mu(E^n)u_i^n + \alpha^{n-1}\mu(E^{n-1})u_i^{n-1}}{d+1} + \phi_i^{E,\mathrm{sN}} - \frac{\sum_{j\in E} u_j^{n+1}}{d+1}\frac{\alpha^{n+1}\mu(E^{n+1}) + \alpha^n\mu(E^n) + \alpha^{n-1}\mu(E^{n-1})}{d+1}. \quad (21)$$

Here $\phi_i^{E,\mathrm{sN}}$ is the well known nodal contribution from the *steady* version of the N scheme

$$\phi_i = k_i^+(u_i - u_{\mathrm{in}}), \qquad u_{\mathrm{in}} = -N\sum_{j\in E} k_j^- u_j, \quad (22)$$

The N scheme is a first order positive scheme, if a proper time discretization formula is used.

The schemes are extended to the system of Euler equations following the approach of [23].

A second order non-oscillatory scheme for the Euler equations can be constructed by using a blending coefficient $\theta = \min(1, sc^2\, h)$, $sc = (\frac{\partial p}{\partial t} + \nabla_x p \cdot \vec{v})^+/\delta_{pv}$, where $\vec{v}$ is the velocity vector of the flow, p is the static pressure, h the diameter of the element and δ_{pv} is a product of the characteristic pressure and velocity in the domain. Finally, the sum of the element contributions to each node is driven towards zero using a dual-time approach.

A second option to construct a second order nonlinear scheme is by the modification procedure, where the (implicitly defined) distribution coefficients are limited, such that they become uniformly bounded, see e.g. [18]. The scheme is called N-modified scheme.

5 Finite volume scheme

The idea behind the finite volume schemes, i.e. approximating the integral of the divergence terms as a contour integral, has contributed to the development of many numerical methods, see e.g. [22]. This part of the work is devoted to finite volume methods as defined in [12], i.e. discretizations based on eq. (24). Such discretization will be referred to as a *finite volume method*.

The domain of solution Ω is covered by a mesh consisting of elements. We consider two classes of FV schemes: cell centered (CC) and vertex centered (VC), see [3, 12]. For the CC method the (finite) volume used to satisfy the integral form of the equation is the mesh element itself, while for the VC method the finite volumes are cells of the dual mesh. Dual cells are constructed in two dimensions by connecting the centroids of the mesh elements with the centers of the edges. A similar construction applies in 3D.

We start from the conservative ALE formulation (1). The equation is integrated over finite element E_i. Using the Gauss-Ostrogradski theorem, the mean value theorem and the substitution theorem we get a relation between the mean value of the time derivative in the finite volume and the contour integral of convective terms

$$\left.\frac{\partial J_{\mathcal{A}_t}\mathbf{u}}{\partial t}\right|_{\vec{Y}} + \oint_{\partial E_i} [\vec{\mathbf{f}}(\mathbf{u}) - \mathbf{u}\vec{w}] \cdot \mathrm{d}\vec{n} = 0, \tag{23}$$

where $\mathbf{u}_i$ is the mean value of the solution in the element. The contour integral involves the flux on the boundary of the finite volume. It is approximated using the numerical flux evaluated in Gauss points. For the second order approximation, one Gauss point in the centroid of each face of the finite volume is needed.

$$\frac{\partial \mu(E_i)\mathbf{u}_i}{\partial t} + \sum_{\forall j} \mathbf{F}(\mathbf{u}_{L,j}, \mathbf{u}_{R,j}, \vec{n}_j, \vec{w}) = \mathbf{0}, \tag{24}$$

where the index j goes over the faces of the finite volume E_i and $\vec{n}_j$ is the normal of the face scaled by the measure (surface) of the face j. The $\mathbf{u}_{L,j}$ and $\mathbf{u}_{R,j}$ are values of the approximation of the solution at the Gauss point from the left and right side of the face of the finite volume. The ALE flux is computed using a modification of Roe's approximated Riemann solver [19]. The face velocity $\vec{w}$ and the (time dependent) normal $\vec{n}_j$ are approximated as in [11].

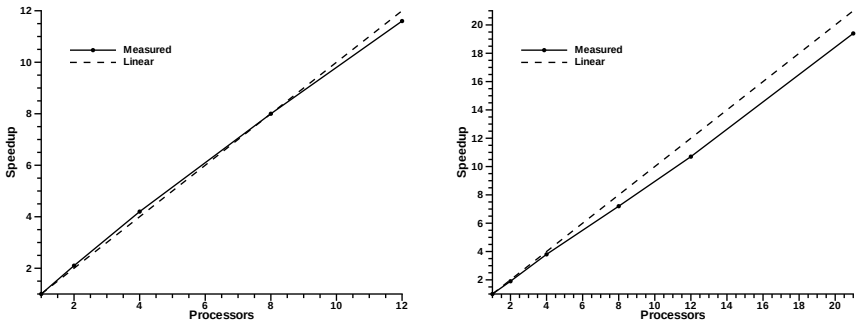

Figure 1: Onera M6 wing 5×306843 DOF. WLSQR reconstruction. Parallel speed-up. Left: explicit scheme. Right: implicit scheme, $CFL = 1000$.

In order to increase the accuracy of the method, linear reconstruction in each control volume is applied. To preserve non-oscillatory properties of the method we use Barth limiter [4] or WLSQR approach [10].

The problem is solved in dual time in parallel. The computational domain is split in (almost) equal size sub-domains. The problem is then distributed to different processors in the computational cluster. The data are interchanged with help of the MPI library. The same approach is used also for the residual distribution schemes.

6 Comparison of some FV and RD schemes

In this section we shall investigate finite volume (FV) schemes both in vertex centered (VC) and cell centered (CC) settings in comparison with residual distribution (RD) schemes. To perform such a comparison one has to overcome a number of technical problems.

- Cell and vertex centered methods employ a different number degrees of freedom for the same mesh.
- The methods can significantly differ in their computational complexity.
- The methods have to be available with similar level of development maturity (i.e. both state–of–the–art FV and RD codes).

- Formulation and implementation of the boundary conditions can significantly affect the solution.

Up-to now, there is no wide agreement on the definite superiority of one type of method.

We have selected a number of test cases examinating different aspects of the schemes. The test cases are sorted from easy to more complex: from scalar linear equation, then scalar nonlinear equation up-to the system of nonlinear equations; from steady to unsteady flow; from smooth solution to discontinuous solution.

To enable comparison of the methods with different number of degrees of freedom, i.e. cell centered and vertex centered methods, we define an equivalent mesh spacing

$$h^{\mathrm{ball,2D}} = 2\sqrt{\frac{S_i}{\pi}}, \quad h^{\mathrm{ball,3D}} = \sqrt[3]{\frac{3}{4}\frac{S_i}{\pi}}, \tag{25}$$

where h^{ball} is the diameter of circle (ball) with surface (volume) S_i, with

$$S_i = \frac{\mu(\Omega)}{\mathrm{DOF}}. \tag{26}$$

The surface of the whole computational domain is denoted by $\mu(\Omega)$ and DOF is the number of degrees of freedom in the domain.

As the first test, we solve the steady scalar advection equation introduced in section 3 on a domain $\Omega = [-1, 1] \times [0, 1] \times [0, 1]$, with the initial conditions $u^0 = 0$ and boundary conditions

$$u = \begin{cases} \cos^2[\pi \min(0.5, 1.4\,\|\vec{x} - (0.5, 0, 0.5)\|)] & \text{on } x > 0,\ y = 0, \\ 0 \qquad \text{on the rest of inflow boundary.} \end{cases} \tag{27}$$

The norm of the error with respect to the equivalent mesh spacing is plotted in Fig. 2. One can observe high accuracy of the LDA scheme in comparison with all the other schemes. The order of convergence for a similar 2D problem computed from a mesh refinement study is given in Tab. 3. A second order convergence rate is observed for linear FV schemes with linear reconstruction and for the LDA scheme in relevant norms.

The next test case examines the accuracy of the numerical methods on deforming meshes. It is probably the most important test case in this thesis, because proper extension of unsteady schemes for moving mesh computations always raises accuracy concerns [7]. The LDA scheme is compared with the

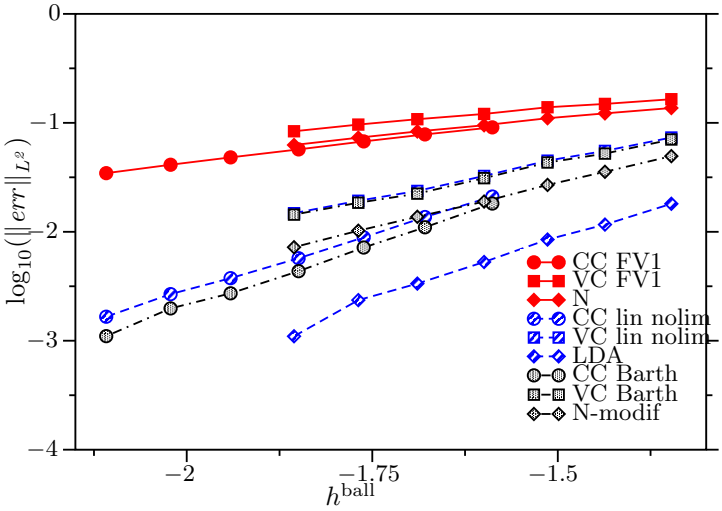

Figure 2: 3D steady circular advection problem. Convergence study.

FV scheme. The FV scheme uses linear reconstruction without limiter. Both schemes are equipped with the 3BDF time integrator. The setup of the test-case is similar as for the previous test. We solve the problem on a square $\Omega = [-1, 1] \times [-1, 1]$. As the initial condition the following cosine profile was prescribed

$$u^0(\vec{x}) = 1 + \frac{\cos(4\pi \min(d, 1/4))}{2}, \qquad d = \|\vec{x} - (-0.5, 0)\|. \tag{28}$$

The mesh coordinates depend on time with formula

$$\vec{x}(t) = \frac{3 - \cos t}{2} \vec{Y}, \tag{29}$$

where $\vec{Y}$ is the original mesh coordinate and $\vec{x}(t)$ is the current configuration mesh coordinate. The error is measured in L^p norm over the space-time domain $\Omega_t \times [0, 2\pi]$. The convergence is plotted in Fig. 4 and the rate of convergence is computed from the least square fit in tab below. Both schemes give almost second order accuracy. The higher accuracy of the LDA scheme in comparison with the FV scheme is clear, both from the lower error and from the higher convergence rate.

Scheme	L^1 order	L^2 order	L^∞ order
CC FV Const.	0.76	0.72	0.60
VC FV Const.	0.58	0.54	0.40
N	0.75	0.71	0.59
CC FV Linear	2.04	1.92	0.90
VC FV Linear	1.99	1.95	1.39
LDA	2.16	2.11	1.79
CC FV Barth	1.64	1.60	0.96
VC FV Barth	2.00	1.95	1.47
N-mod	1.66	1.54	1.21

Figure 3: 2D steady circular advection problem. Estimated order of accuracy.

A comparison of the methods for transonic flow past the Onera M6 wing is presented as the next test case, see [21]. We have chosen data from Test 2308, i.e. with free stream Mach number $Ma_\infty = 0.8395$ and angle of attack $\alpha = 3.06^\circ$. We use an unstructured mesh consisting of 57041 nodes and 306843 tetrahedral elements. This means that the CC FV scheme cannot be directly compared to the VC FV and RD schemes, since the CC FV uses about 6 times more unknowns. Isolines of the Mach number are presented in Fig. 5. The λ-shock pattern is clearly visible for the more accurate schemes. Comparison with experimental data is presented.

In order to asses the performance of the scheme for Euler equations on deforming meshes, we present a test case consisting of a compression of gas inside a cylindrical piston. The test case is essentially one-dimensional, however we solve the problem in three dimensions. The domain is initially of length 5, with diameter of 1. The initial state is defined by $\rho_0 = 1.4$, $p_0 = 1$ and zero velocity. The gas is enclosed with walls. The wall $x_0 = 0$ starts to accelerate with derivative of acceleration $\dddot{x} = 0.2$, while the opposite wall is fixed. The position of the nodes in between is linearly interpolated. The simulation is performed until time $t = 4$. The problem can be solved analytically by a method of characteristics. We use a fully unstructured mesh consisting of 3257 nodes and 16054 tetrahedral elements. Note that the FV scheme uses rougly 6$\times$ more DOF than the RD method. The mesh plot with isolines of Mach number for time $t = 4$ ($\Delta t = 0.04$) is presented in Fig. 6, top. One can observe that the isolines are essentially straight lines. The distribution of the pressure and density along the x axis is shown in the middle and bottom *for*

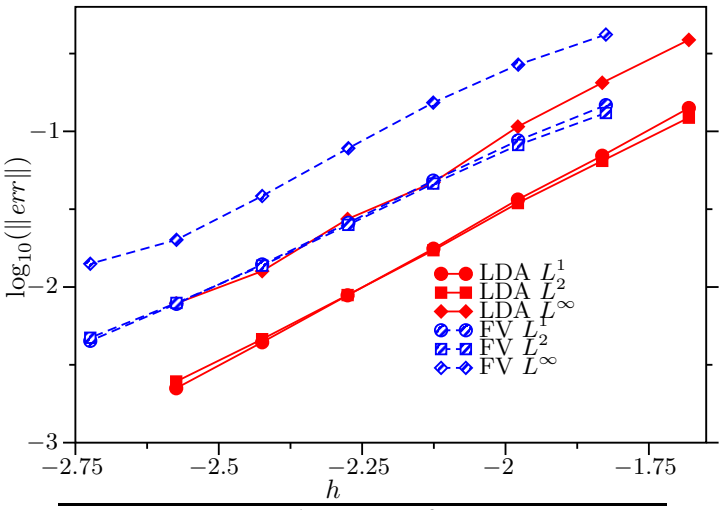

Scheme	L^1 order	L^2 order	L^∞ order
LDA	2.02	1.91	1.94
CC FV2 nolim	1.71	1.64	1.73

Figure 4: 2D unsteady circular advection problem of deforming mesh. LDA scheme and FV scheme with linear reconstruction without limiter. Norm of error vs. mesh spacing and estimated order of accuracy.

all the nodes in the computational domain. In both cases a more accurate behavior of the LDA scheme compared to the FV scheme can be seen.

7 Finite element method for elasticity problems

In this section we will formulate the elastic problem and state the numerical method. The strain tensor for large displacements has the form

$$\varepsilon_{ij} = \frac{1}{2}\left(\frac{\partial u_i}{\partial x_j} + \frac{\partial u_j}{\partial x_i} + \frac{\partial u_k}{\partial x_i}\frac{\partial u_k}{\partial x_j}\right), \tag{30}$$

where u_j is the displacement in direction j and k is a summation index. The quadratic term renders the method nonlinear. The displacement is defined

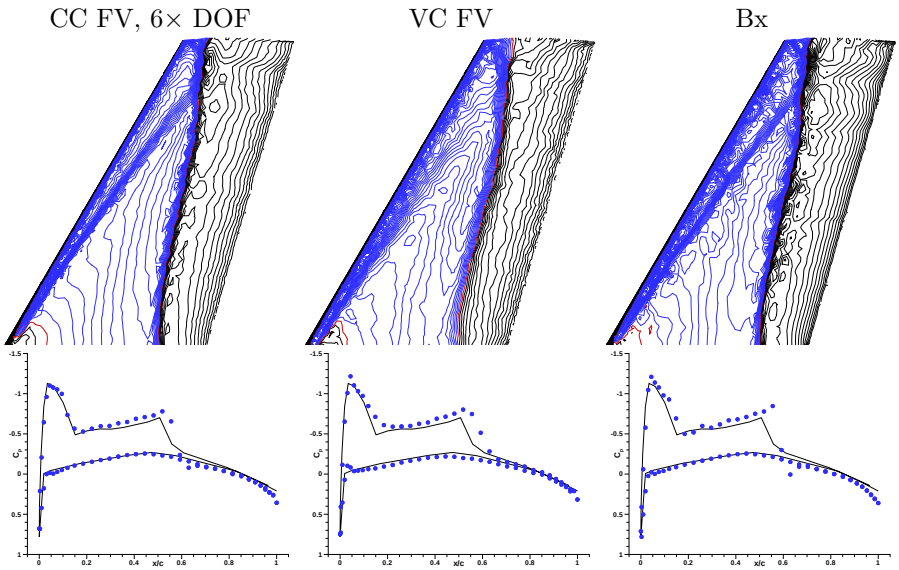

Figure 5: Inviscid flow past Onera M6 wing. Isolines of Mach number and the pressure coefficient at 44 % of span. Full line: experiment, points: numerical solution. Left: CC FV WLSQR scheme. Middle: VC FV WLSQR scheme. Right RD Bx scheme.

as the difference between the deformed state and the initial state

$$u_i = x'_i - x_i. \tag{31}$$

We use a linear relation between the strain ε and the stress σ called (generalized) Hooke's law

$$\sigma_{ij} = c_{ijkl}\varepsilon_{kl}, \tag{32}$$

where c_{ijkl} is the elastic tensor. The dynamic equation for the continuum (Newton's law) is

$$\rho\frac{\partial^2 u_i}{\partial t^2} = \frac{\partial \sigma_{ij}}{\partial x_j} + f_i, \tag{33}$$

where f_i is a component of the internal force (e.g. gravity) and ρ is the material density. Structural damping is not considered.

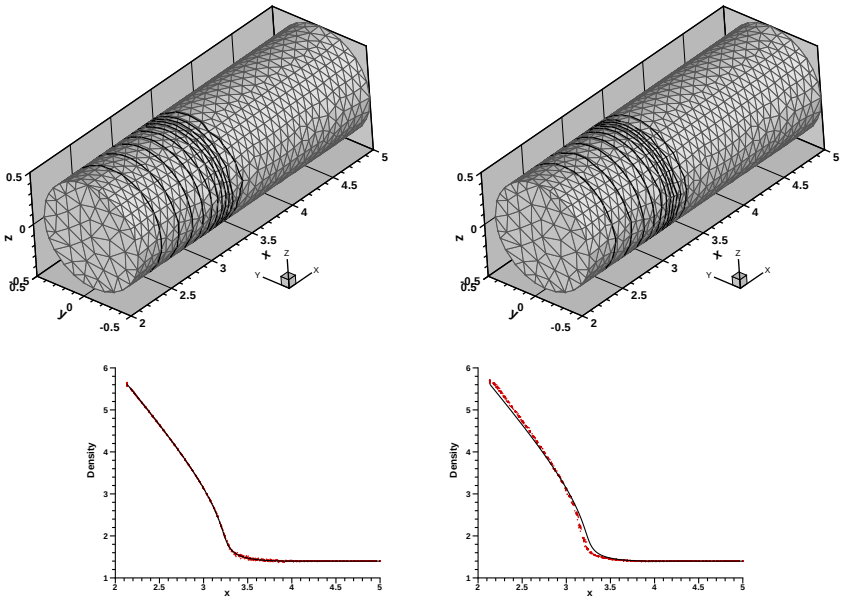

Figure 6: Piston driven compression, solution at $t = 4$. Left column: LDA scheme. Right column: FV scheme. Top row: Isolines of Mach number and computational mesh. Middle and Bottom rows: Dots represent pressure and density as a function of x, plotted for all points in the computational domain. Full line: exact solution. Note that the FV scheme uses rougly $6\times$ more DOF than the RD method.

Multiplying (33) by test function φ and integrating over Ω we obtain the weak form of the equation,

$$\int_\Omega \varphi\rho\frac{\partial^2 u_i}{\partial t^2}\,\mathrm{d}\Omega + \int_\Omega \frac{\partial\varphi}{\partial x_j}\sigma_{ij}\,\mathrm{d}\Omega = \int_\Omega \varphi f_i\,\mathrm{d}\Omega + \oint_{\partial\Omega}\varphi\, t_i\,\mathrm{d}S, \qquad (34)$$

where t_i is a traction (load per unit surface) in the direction of the i axis. This formulation leads directly to the matrix representation for the numerical method.

The domain of solution is covered by finite elements. The displacement u_i

Figure 7: Finite elements in 2D. Left: linear TRI3 element. Middle: bilinear QUAD4 element. Right: biquadratic sub-parametric element QUAD9, the solution is approximated with 9 DOF, the geometry with 4 DOF.

in the i-direction is approximated by the trial functions as

$$u_i^h = \sum_{k \in \mathcal{T}^h} u_{i,k} \psi_k. \tag{35}$$

The trial functions depend on the element used. (We use Lagrangian P1, Q1 and Q2 elements as depicted in Fig. 7.) As we use the Galerkin method, the test functions belong to the same space as the trial functions. The weak formulation (34) gives directly the finite element method, where the solution is replaced by its approximation (35) and the test functions by φ_k. The problem can be written as

$$\mathbf{M}\ddot{U} + \mathbf{K}U = F, \tag{36}$$

where U is the algebraic vector of unknowns (displacements), $\mathbf{M}$ is the mass matrix, $\mathbf{K}$ is the stiffness matrix and F the vector of right hand sides.

For the time integration we have chosen the Newmark method. We have also included modal analysis capabilities, where we solve a generalized eigenproblem

$$\omega_m^2 \mathbf{M} U_m + \mathbf{K} U_m = 0. \tag{37}$$

8 Numerical method for fluid–structure interaction

In this section a method to couple both problems will be discussed. We use a three field formulation introduced in [13]. The three distinct fields involve computational fluid dynamics (CFD), computational structural mechanics (CSM) and the fluid mesh deformation as the third field.

- CFD is coupled with the CSM via position and velocity of the computational domain. It is also intrinsically coupled to the mesh dynamics.
- CSM is coupled to CFD by the stress tensor on the surface of the body.
- The position and velocity of the fluid mesh boundary is coupled to the position and velocity of the surface of the body. The force acting to the elastic body is related to the pressure of the fluid at the boundary.

For the aeroelastic computations, there is a strong need to treat nonmatching interfaces. We compute the displacement of the fluid boundary nodes as follows: we project the fluid boundary nodes to the elastic boundary. We compute the value of the finite element trial functions at the projected point. The fluid boundary displacement is given by the weighted average of the nodal displacements given at the elastic boundary nodes, where the weights are given by the finite element trial functions.

The force on the boundary of the elastic body is prescribed from the equality of virtual work. The virtual work performed by the fluid boundary has to be equal to the virtual work of the elastic boundary

$$\int_{\Gamma_F} -p\,\vec{n}\cdot\vec{u}_F\,\mathrm{d}s = \sum_{i=1}^{i=i_S} \vec{f}_i\cdot\vec{u}_{S_i}. \tag{38}$$

Considering how the displacement of the fluid boundary was determined, is is possible to evaluate the force acting at the elastic boundary nodes as the weighted sum of the pressure forces acting on the fluid boundary. In this case, the energy exchanged between the elastic body and fluid domain is conserved.

As a simplification in 2D, we also consider the body motion governed by two ordinary differential equations.

9 Numerical results of fluid–structure interaction problems

We consider supersonic panel flutter, see [17]. An elastic panel with infinite aspect ratio is clamped on both edges. Its upper side is exposed to a supersonic air-stream, while the lower side resides in the still air with the same pressure as on the upper side. The panel has length $L = 0.5\,\mathrm{m}$, a uniform

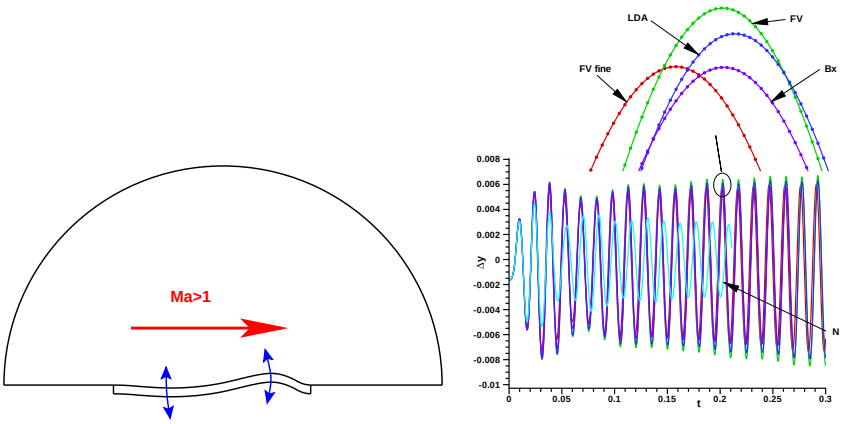

Figure 8: Panel flutter problem. Dependence of the integral of deflection on time for different numerical schemes. $Ma_\infty = 2.2$.

thickness $h = 1.35{\cdot}10^{-3}\,\mathrm{m}$, Young modulus $E = 7.728{\cdot}10^{10}\,\mathrm{N/m^2}$, Poisson ration $\nu = 0.33$ and density $\rho_s = 2710\,\mathrm{kg/m^3}$. The plane strain assumption was used. The flow conditions are given by $p_\infty = 25714\,\mathrm{Pa}$ and $\rho_\infty = 0.4\,\mathrm{kg/m^3}$. The critical Mach number Ma_∞^{cr}, that is, the lowest free stream Mach number for which an unstable aero-elastic mode of the panel appears, is given in the reference [17]. Using theoretical methods (linearized theory) the authors get $Ma_\infty^{\mathrm{cr}} \approx 2.27$ and using their numerical scheme $Ma_\infty^{\mathrm{cr}} \approx 2.23$, what they consider an "excellent agreement".

The elastic panel is discretized with 60×2 elements. The computational domain is formed by a half-circle of diameter $R = 5$. The mesh consists of 3451 nodes and 6722 triangular elements, giving 50 elements along the panel. One more computation is performed on a regular quadrilateral mesh of 300×100 elements with 100 elements along the panel (referred as "fine"). The integral of the deflection of the panel for $Ma = 2.2$ is plotted in Fig. 8. The neutral response was correctly reproduced. Although the LDA scheme is a linear scheme, it is able to capture weak shock waves in a non-oscillating manner. The nonlinear Bx scheme gives similar results as the LDA scheme, which are very different from the first order N scheme.

Finally, transonic flutter of the AGARD 455.6 wing ("solid model") is considered [6]. The elastic wing was discretized using 350 tri-quadratic elements. The CFD mesh consists of 22k nodes and 118k tetrahedral elements. The

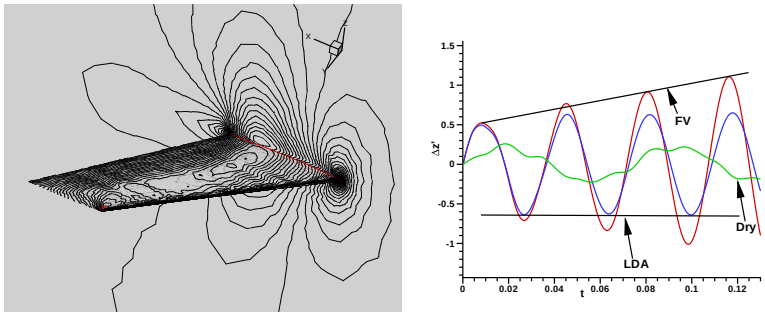

Figure 9: AGARD 445.6 wing. Time dependence of the volume integral of the wing velocity for the measured neutral response regime.

neutral response regime was chosen, which is characterized by the flutter speed index of 0.5214 and the free stream Mach number $Ma_\infty = 0.92$ with flow medium Freon-12. One period was divided in 120 time-steps. The integral of the wing deflection is plotted in Fig. 9. For the FV scheme, a small negative damping is observed, while for the LDA scheme the neutral response was correctly reproduced. The difference between the measured oscillation period and the computed period is 0.66 % for the LDA scheme and 2.08 % for the FV scheme. Considering the uncertainty of the elastic constants we judge this result more accurate than one can expect.

10 Conclusions

The goals stated in the beginning of presented work were successfully fulfilled.

1. A numerical method based on residual distribution schemes was developed and several extensions for moving mesh simulation were proposed. We have analyzed the positivity of first order schemes, showing that the proposed extension satisfies a discrete maximum principle for a scalar conservation law. We have also analyzed the positivity and accuracy requirements of nonlinear schemes constructed as a linear combination of low and high order schemes. We have proposed and tested a new nonlinear scheme built as a convex combination of the LDA and the N scheme, named Bx scheme.

2. We have developed a finite volume method in both cell centered and ver-

tex centered settings, including the capability to handle moving meshes. We have tested the influence of renumbering degrees of freedom for a parallel implicit method, showing its importance for the parallel performance.

3. We have conducted a number of computational experiments, starting from scalar advection problems, Burgers equation to the Euler equations, including the technically important case of transonic flow past the Onera M6 wing. The tests were performed in two and three spatial dimensions, for steady and unsteady problems, including problems with deforming meshes. A number of convergence studies for scalar cases were performed, also in three dimensions, giving opportunity to directly compare accuracy of different schemes for the same test case.

4. A finite element method for the structural problem has been developed in two and three dimensions including large displacement formulation and handling of anisotropic material properties. The modal analysis capabilities were included, as they are needed for the validation of the structural model and the prescription of the initial conditions in the fluid–structure interaction problem.

5. A numerical method for fluid–structure interaction was developed and coded. The numerical method for the fluid flow is based on the schemes developed in the first part of the work. Interface boundary conditions were developed and validated. The mesh motion algorithm uses the finite element method to find a nodal displacement. The method was validated for 2D transonic flow past a NACA 64A010 airfoil, where the structural dynamics is modeled by a system of two ordinary differential equations. The flutter, neutral and damping response were correctly reproduced. A flutter boundary for one selected Mach number of a two-dimensional elastic panel problem was computed and compared with theoretical results and solutions known from the literature. Finally, the method was tested on the 3D AGARD 445.6 wing test case. We have compared the solution using different developed CFD methods, both of the residual distribution and finite volume type.

References

[1] R. Abgrall and M. Mezine. Construction of second order accurate monotone and stable residual distribution schemes for unsteady flow problems. *Journal of Computational Physics*, 188:16–55, 2003.

[2] A. Athanasiadis. *Three-dimensional hybrid grid generation with application to high Reynolds number viscous flows*. PhD thesis, Université Libre de Bruxelles, Von Karman Institute for Fluid Dynamics, 2005.

[3] T. J. Barth and M. Ohlberger. *Encyclopedia of Computational Mechanics*, volume 1, Fundamentals, chapter Finite Volume Methods: Foundation and Analysis. John Wiley and Sons, Ltd, 2004.

[4] T. J. Barth. Aspects of unstructured grids and finite-volume solvers for the Euler and Navier-Stokes equations. In *25th Computational Fluid Dynamics*. von Karman Institute, Mar 1994.

[5] H. Deconinck, P. L. Roe, and R. Struijs. A multidimensional generalization of Roe's flux difference splitter for the Euler equations. *Computers and Fluids*, 22:215–222, 1993.

[6] J. E. Carson Yates. AGARD standard aeroelastic configurations for dynamic response. Candidate configuration I.-Wing 445.6. Technical Memorandum 100492, NASA, August 1987.

[7] C. Farhat. *Encyclopedia of Computational Mechanics*, chapter CFD-Based Nonlinear Computational Aeroelasticity. John Wiley & Sons, Ltd., 2004.

[8] A. Ferrante and H. Deconinck. Solution of the unsteady Euler equations using residual distribution and flux corrected transport. Project Report VKI PR 1997-08, Von Karman Institute for Fluid Dynamics, Belgium, June 1997.

[9] L. Formaggia and F. Nobile. Stability analysis of second-order time accurate schemes for ALE-FEM. *Comput. Methods Appl. Mech Engrg.*, 193:4097–4116, 2004.

[10] J. Fürst. A weighted least square scheme for compressible flows. *Flow, Turbulence and Combustion*, 76(4):331–342, June 2006.

[11] B. Koobus and C. Farhat. Second-order time-accurate and geometrically conservative implicit schemes for flow computations on unstructured dynamic meshes. *Comput. Methods Appl. Mech. Engrg.*, 170(1–2):103–129, 1999.

[12] D. Kröner. *Numerical Schemes for Conservatino Laws*. John Wiley & Sons Ltd., 1997.

[13] M. Lesoinne and C. Farhat. Stability analysis of dynamic meshes for transient aeroelastic computations. AIAA Paper 93-3325, AIAA, 1993. 11th AIAA Computational Fluid Dynamics Conference, July 6–9, Orlando, Florida.

[14] C. Michler, H. D. Sterck, and H. Deconinck. An arbitrary Lagrangian Eulerian formulation for residual distribution schemes on moving grids. *Computers and Fluids*, 32(1):59–71, 2003.

[15] R. H. Ni. A multiple grid scheme for solving Euler equations. *AIAA Journal*, 20(1), 1981.

[16] H. Paillère. *Multidimensional Upwind Residual Distribution Schemes for the Euler and Navier-Stokes Equations on Unstructured Grids*. PhD thesis, Université Libre de Bruxelles, Von Karman Institute for Fluid Dynamics, June 1995.

[17] S. Piperno and C. Farhat. Partitioned procedures for the transient solution of coupled aeroelastic problems part II: Energy transfer analysis and three-dimensional applications. *Comput. Meths. Appl. Mech. Engrg.*, 190(24):3147–3170, 2001.

[18] M. Ricchiuto, A. Csík, and H. Deconinck. Residual distribution for general time-dependent conservation laws. *Journal of Computational Physics*, 209(1):249–289, 2005.

[19] P. L. Roe. Approximate Riemann solvers, parameter vectors, and difference schemes. *J. Comput. Phys.*, 43:357–372, 1981.

[20] P. L. Roe. Fluctuations and signals – a framework for numerical evolution problems. In K. W. Morton and M. J. Baines, editors, *Numerical Methods for Fluid Dynamics*, pages 219–257. Academic Press, 1982.

[21] V. Schmitt and F. Charpin. Pressure distributions on the Onera–M6–wing at transonic Mach numbers. Advisory Report AGARD-AR-138, Advisory Group for Aerospace Research & Development, 1979.

[22] E. Stein, R. de Borst, and T. J. R. Huges, editors. *Encyclopedia of Computational Mechanics*. John Wiley & Sons, Ltd., 2004.

[23] E. T. A. van der Weide. *Compressible Flow Simulation on Unstructured Grids Using Multi-dimensional Upwind Schemes*. PhD thesis, Technische Universiteit Delft, Von Karman Institute for Fluid Dynamics, 1998.

Some publications related to the presented results

[1] H. Deconinck, R. Abgrall, M. Ricchiuto, K. Sermeus, T. Wuilbaut, J. Dobeš, and N. Villedieu. A class of conservative residual discretizations for solving convervation laws on unstructured meshes. Invited Lecture. EUA4X training course & 34th VKI CFD Lecture series. Von Karman Institute. Belgium, 2005.

[2] H. Deconinck, M. Ricchiuto, J. Dobeš, and K. Sermeus. A class of conservative residual discretizations for solving convervation laws on unstructured meshes. Invited Lecture. ACOMEN 2005. Gent, Belgium, 2005.

[3] J. Dobeš and H. Deconinck. Second order blended multidimensional residual distribution scheme for steady and unsteady computations. *Journal of Computational and Applied Mathematics (JCAM)*, 2005. Accepted.

[4] J. Dobeš and H. Deconinck. A second order space-time residual distribution method for solving compressible flow on moving meshes. AIAA Paper 2005–0493, American Institute of Aeronautics and Astronautics, 2005. Also avaliable as: 2005 AIAA Meeting Papers on Disc, Vol. 10, No. 1-4, Conference Proceeding Series [CD-ROM]. ISBN 1-56347-757-2.

[5] J. Dobeš, H. Deconinck, and J. Fořt. Arbitrary Lagrangian Eulerian formulation: Lax-Wendroff type theorem and convergence study for residual distribution method. *International Journal for Numerical Methods in Fluids*, 2007. Submitted.

[6] J. Dobeš, H. Deconinck, and J. Fořt. Design of unsteady nonlinear multidimensional residual distribution schemes – application for moving meshes problems. *Computers and Fluids*, 2007. To appear.

[7] J. Dobeš, J. Fořt, J. Fürst, J. Halama, T. Hyhlík, P. Louda, K. Kozel, J. Příhoda, and P. Šafařík. Experimental and numerical analysis of transonic flow through plane turbine cascade. *Engineering Mechanics*, 10(5), 2003. ISSN 1210-2717.

[8] J. Dobeš, J. Fořt, J. Fürst, J. Halama, and K. Kozel. Numerical solution of transonic flows in a 2D and 3D axial and radial turbine cascades. In J. V. T. Lajos, editor, *Proceedings of "Modelling Fluid Flow" (CMFF'03)*, volume II, pages 1230–1237, Budapest, September 2003. ISBN 96342077740.

[9] J. Dobeš, J. Fořt, J. Fürst, J. Halama, and K. Kozel. Numerical solution of transonic flows in turbine cascades. In *1st International Conference "From Scientific Computing to Computational Engineering"*. University of Patras, 2004.

[10] J. Dobeš, J. Fořt, J. Fürst, J. Halama, and K. Kozel. Numerical solution of transonic flows in turbine cascades. In *Proceedings of Conference "International Conference "From Scientific Computing to Computational Engineering", 8–10 September, Athens*, 2004.

[11] J. Dobeš, J. Fořt, and J. Halama. Numerical solution of transonic turbulent and two-phase flow in turbine cascades. *PAMM*, 3(1):404–405, 2003.

[12] J. Dobeš, J. Fořt, and J. Halama. Numerical solution of single- and two-phase transonic flow in axial cascade. In *Proceedings of 4th European Congress on Computational methods in Applied Sciences and Engineering*, volume 1. University of Jyvaskyla, 2004. ISBN 951-39-1868-8.

[13] J. Dobeš, J. Fořt, and J. Halama. Numerical solution of single and multiple-phase internal transonic flow problems. *International Journal for Numerical Methods in Fluids*, 48(1):91–97, March 2005.

[14] J. Dobeš, J. Fürst, and H. Deconinck. Convergence analysis of arbitrary lagrangian eulerian formulation for residual distribution schemes. In *ICFD conference "Numerical Methods for Fluid Dynamics"*, 2007. To appear.

[15] J. Dobeš, J. Fürst, J. Fořt, J. Halama, and K. Kozel. Numerical simulation of transonic flow in steam turbine cascades. In H. Sobieczky, editor, *Proceedings of Symposium Transonicum IV*, pages 145–150, Göttingen, September 2002. DLR, Kluwer Academic Publishers. ISBN 1-4020-1608-5.

[16] J. Dobeš, J. Fürst, J. Fořt, J. Halama, and K. Kozel. Numerical solution of transonic flows in 2D and 3D axial and radial turbine cascades. In *Proceedings of 5th European conference on Turbomachinery*, pages 1105–1114, Prague, 2003.

[17] J. Dobeš and H. Deconinck. An ale formulation of the multidimensional residual distribution scheme for computations on moving meshes. In *4th ICCFD conference*, Gent, Belgium, June 2006. Springer. Accepted.

[18] J. Dobeš and H. Deconinck. A second order unconditionally positive space-time residual distribution method for solving compressible flows on moving meshes. In *Programs and Algorithms of Numerical Mathematics 13*, Mathematical Institute, Academy of Sciences, Žitná 25, Prague, Czech Republic, May 2006.

[19] J. Dobeš and H. Deconinck. A shock sensor based second order blended (Bx) upwind residual distribution scheme for steady and unsteady compressible flow. In *Eleventh International Conference on Hyperbolic Problems. Theory, Numerics, Applications*. École Normale Supérieure de Lyon, Lyon, France, Springer, 2006. To appear.

[20] J. Dobeš, H. Deconinck, and J. Fořt. Comparison of cell centered and vertex centered formulation of finite volume method. *Inženýrská mechanika/Engineering Mechanics*, 13(3):191–200, 2006.

[21] J. Dobeš, M. Ricchiuto, and H. Deconinck. *33rd Computational Fluid Dynamics Course – Novel methods for solving convection dominated systems*, chapter Implicit Space-Time Residual Distribution Method for Unsteady Laminar Viscous Flow. VKI Lecture Series. Von Karman Institute for Fluid Dynamics, 2003.

[22] J. Dobeš, M. Ricchiuto, and H. Deconinck. Implicit space-time residual distribution method for unsteady viscous flow. In *16th AIAA Computational Fluid Dynamics Conference, Orlando, Florida*, number AIAA 2003–3691, 2003.

[23] J. Dobeš, M. Ricchiuto, and H. Deconinck. Implicit space-time residual distribution method for unsteady laminar viscous flow. *Computers and Fluids*, 34:593–615, 2005. ISSN 0045-7930.

[24] J. Fořt, J. Dobeš, J. Halama, and M. Kladrubský. Upwind and central type schemes applied to internal and external flow problems. *PAMM (Proceedings in Applied Mathematics and Mechanics)*, 1(1):262–263, 2002. ISSN 1617-7061, http://www3.interscience.wiley.com/cgi-bin/abstract/92013333/ABSTRACT.

[25] J. Fořt, J. Fürst, J. Dobeš, J. Halama, and K. Kozel. Numerical solution of transonic flow in se1050 cascade. *PAMM*, 5(1):459–460, 2005.

[26] P. Furmánek, J. Dobeš, J. Fořt, J. Fürst, M. Kladrubský, and K. Kozel. Numerical solution of transonic flows over an airfoil and a wing. In *Conference on Modelling Fluid Flow – CMFF'06*, pages 249–255. Budapest University of Technology and Economics, Department of Fluid Mechanics, 2006.

[27] M. Kolovratník, J. Fořt, P. Šafařík, V. Petr, K. Kozel, J. Dobeš, J. Fürst, J. Halama, and P. Louda. Parní turbína pro energetické bloky s vysokými parametry páry. 1. část. Výzkumná zpráva Z-554/05, České vysoké učení technické v Praze, Fakulta strojní, Ústav mechaniky tekutin a energetiky, Odbor tepelných a jaderných energetických zařízení, 2006.

[28] P. Šafařík, M. Kolovratník, J. Fořt, V. Petr, K. Kozel, P. Louda, J. Fürst, J. Dobeš, and J. Halama. Příspěvek k vývoji parní turbíny s vysokou účinností, Část 2. Výzkumná zpráva Z-197/05, Ústav mechaniky tekutin a energetiky, odbor mechaniky tekutin a termodynamiky, ČVUT Praha, 2005.